Temperature Field beneath Evaporating Surfaces Resolved by Infrared Thermography

Ebrahim Shahraeeni and Dani Or

Soil and Terrestrial Environmental Physics / Swiss Federal Institute of Technology, ETH Zurich

EGU2010 – 3358

Institute of Terrestrial Ecosystems
Soil and Terrestrial Environmental Physics

Eidgenössische Technische Hochschule Zürich
Swiss Federal Institute of Technology Zurich

Abstract

- Land – atmosphere mass exchange is linked with radiation and energy balance of terrestrial surfaces and affected by interplay between water supply from below, surface energy input, and exchange across air boundary layer
- Surface temperature depression of an evaporating surface is proportional to the flux enabling remote monitoring of evaporation by Infrared thermography
- *The objective was to quatify evaporative temperature depression which predicting spatial and temporal evaporation rates distributions based on IRT data*
- We developed a model for evaporation induced temperature field from a patchy evaporative surface and compare the results with IRT data beneath the surface
- Several scales and dimensionless groups controlling evaporation have been introduced based on the mathematical model of the temperature field

Theoretical Considerations

- Surface Energy Balance equation (SEB)

$$\underbrace{\dot{e}(r,t)}_{\text{Evaporation}} = \underbrace{\frac{\Delta h}{\rho_w L_w}\left\{\frac{\varepsilon\sigma\left[T_\infty^4(t)-T^4(r,t)\right]+h\left[T_\infty(t)-T(r,t)\right]}{\Delta h}\right.}_{\text{Radiation + Convection}} \underbrace{-\rho C_p\frac{\partial T}{\partial t}}_{\text{Storage}} \underbrace{\left.-\frac{k_T}{r}\frac{\partial}{\partial r}\left(r\frac{\partial T}{\partial r}\right)\right\}}_{\text{Conduction}} \qquad (1)$$

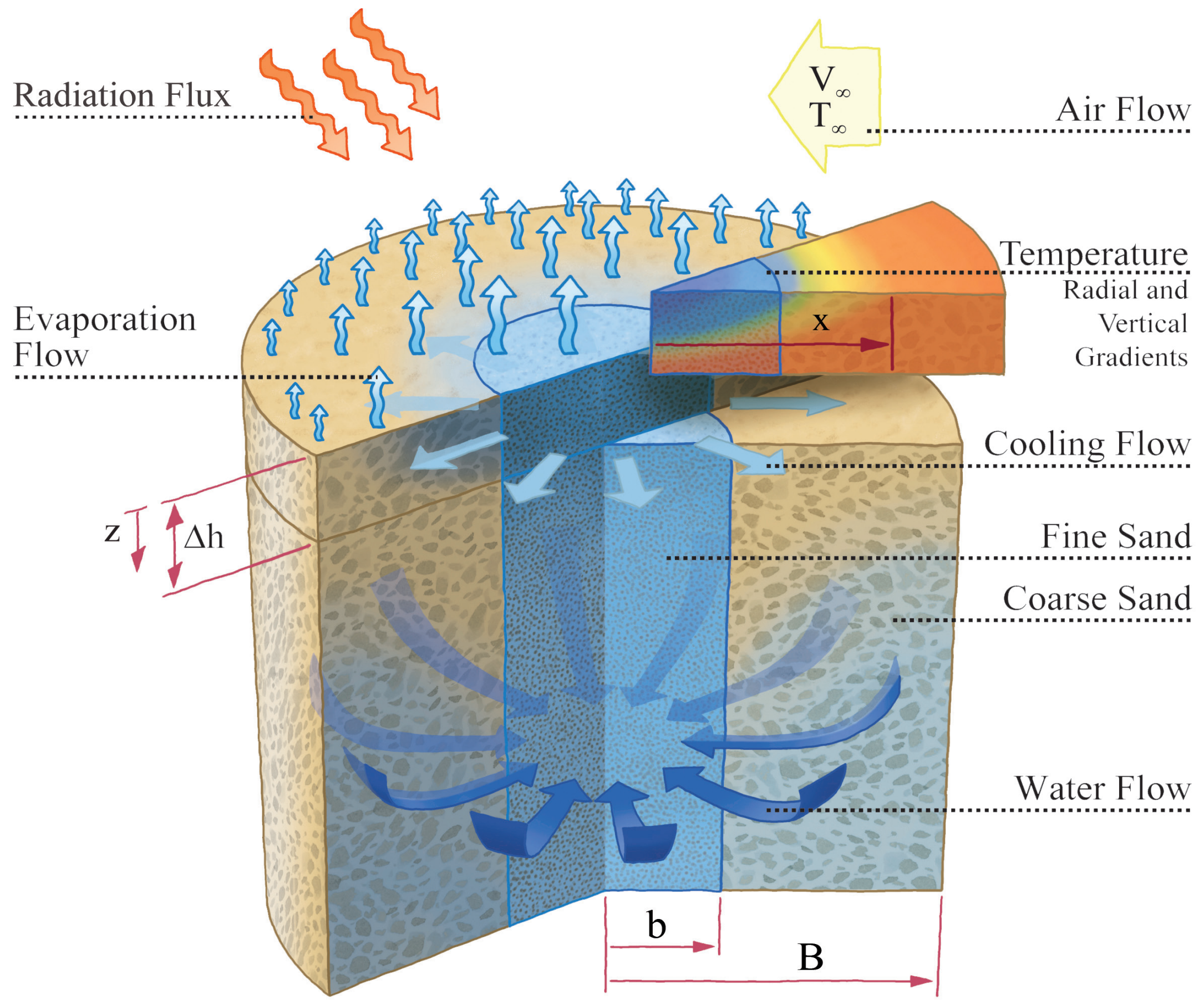

Figure 1: Definition sketch of heat and mass transfer during evaporation from a heterogeneous surface with nonuniform evaporation pattern from top surface.

- The Fourier distribution of surface flux is linked with temperature as:

$$T(x,z)=\sum_{m=0}^{\infty}C_m\exp\left(-\frac{m\pi z}{B}\right)\cos\left(\frac{m\pi x}{B}\right)$$

$$C_m=\begin{cases}\dfrac{\frac{1}{2}k_T a_0}{h+4\sigma\varepsilon T_\infty^3} & m=0\\[2ex] \dfrac{a_m}{\dfrac{m\pi}{B}+\dfrac{h+4\sigma\varepsilon T_\infty^3}{k_T}} & m\neq 0\end{cases}\qquad a_m=\frac{2}{B}\int_0^B\dot{e}(x)\cos\left(\frac{m\pi x}{B}\right)dx \qquad (2)$$

- The physically based model (2) enables determination mass exchange fluxes from temperature distribution of an evaporative surface
- The method is simplified by using mean temperature values for evaporation from heterogeneous surfaces
- The following length scales and dimensionless groups control interactions between various ingredients in SEB equation (1)

$$\dot{e}^*(t)=\frac{\frac{1}{2}\left(\frac{dT_s^*}{dt^*}+Nu_{ext}\overline{T}_s^*\right)}{Nu_{ext}\pm 2Ebr\left(B^*,Nu_{ext}\right)}$$

$$Nu_{ext}=\frac{\textbf{\textit{Convection + Radiation}}}{\textbf{\textit{Conduction}}}=\frac{b\left(h+4\sigma\varepsilon T_\infty^3\right)}{k_T}$$

$$Ebr\left(B^*,Nu_{ext}\right)=\frac{\textbf{\textit{Conduction}}}{\textbf{\textit{Evaporation}}}=\sum_{m=1}^{\infty}\frac{\frac{2Nu_{ext}}{m\pi}\sin^2\left(\frac{m\pi}{B^*}\right)}{\frac{m\pi}{B^*Nu_{ext}}+1}\left[1-\exp\left(-\frac{m\pi}{B^*Nu_{ext}}\right)\right] \qquad (3)$$

$$\Delta h^*=\frac{2.4k_Tb}{h+4\sigma\varepsilon T_\infty^3+\frac{\rho_wL_w\dot{e}}{T_\infty}}\ (\textbf{\textit{Vertical Length scale}})$$

$$\Delta x^*=\frac{Nu_{ext}+2Ebr\left(B^*,Nu_{ext}\right)}{\frac{1}{2}\left(\frac{dT_s^*}{dt^*}+Nu_{ext}T_s^*\right)Ebr\left(B^*,Nu_{ext}\right)}\ (\textbf{\textit{Lateral Length scale}})$$

$$t_0=\frac{\rho c_p b}{h+4\sigma\varepsilon T_\infty^3}\ (\textbf{\textit{Time scale}})$$

Experimental Setup

- FLIR ThermaCAM SC6000 (FLIR, MA, USA, www.flir.com) is the heart of experimental setup for evaporation thermography
- It has been equipped with QWIP detector works in the spectral range of 8 - 9.2μm with the resolution of 640×512 pixel. NETD (Noise Equivalent Temperature Difference) is less than 35mK.

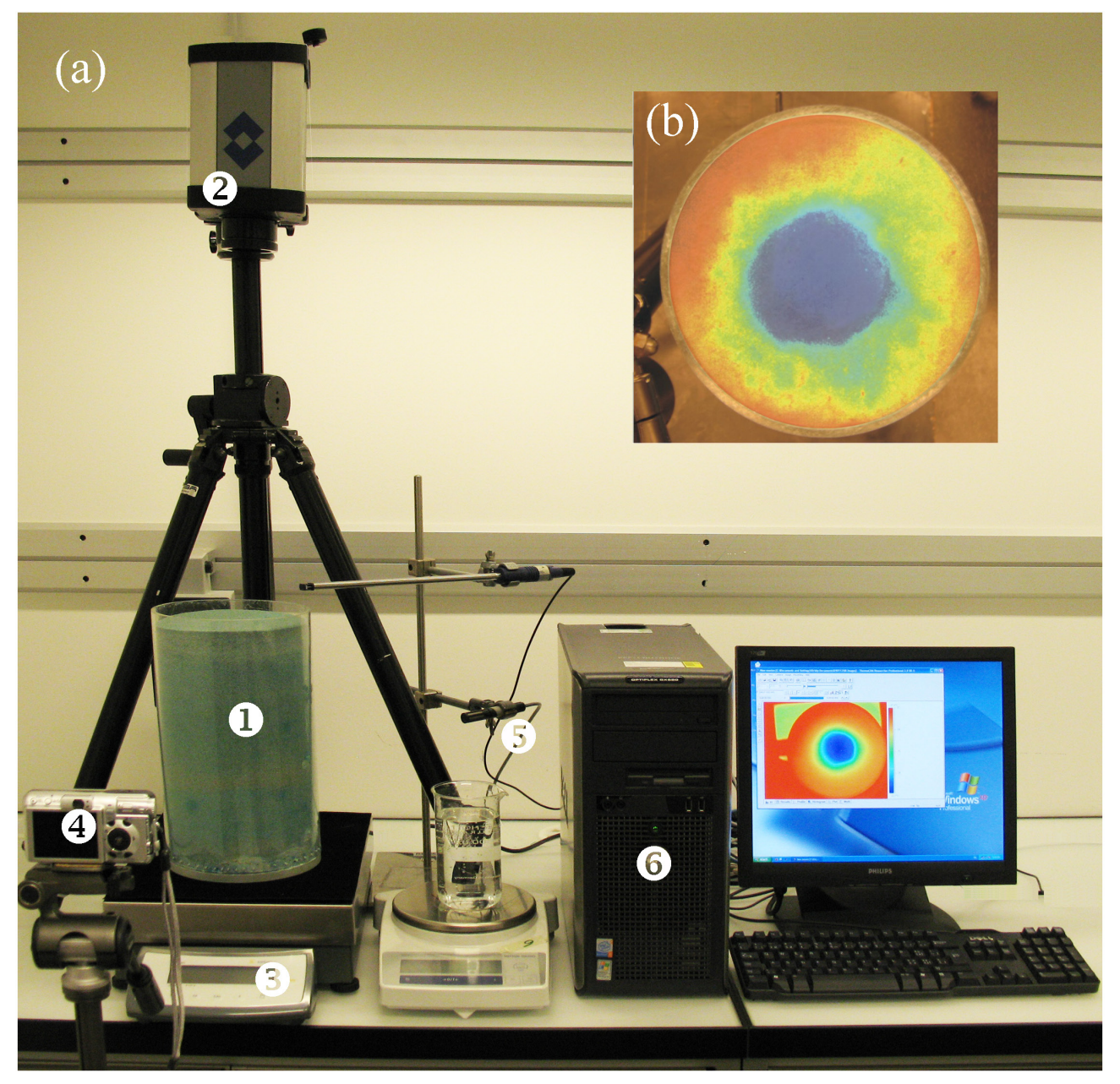

Figure 2: **(a)** Experimental setup for IRT imagery:
(1) Cylindrical Sample
(2) IR camera
(3) Balance (32kg±0.1g)
(4) Normal camera
(5) Ambient Data Recorders
(6) PC for data acquisition and processing
(b) Evaporation from surface with abrupt vertical heterogeneity

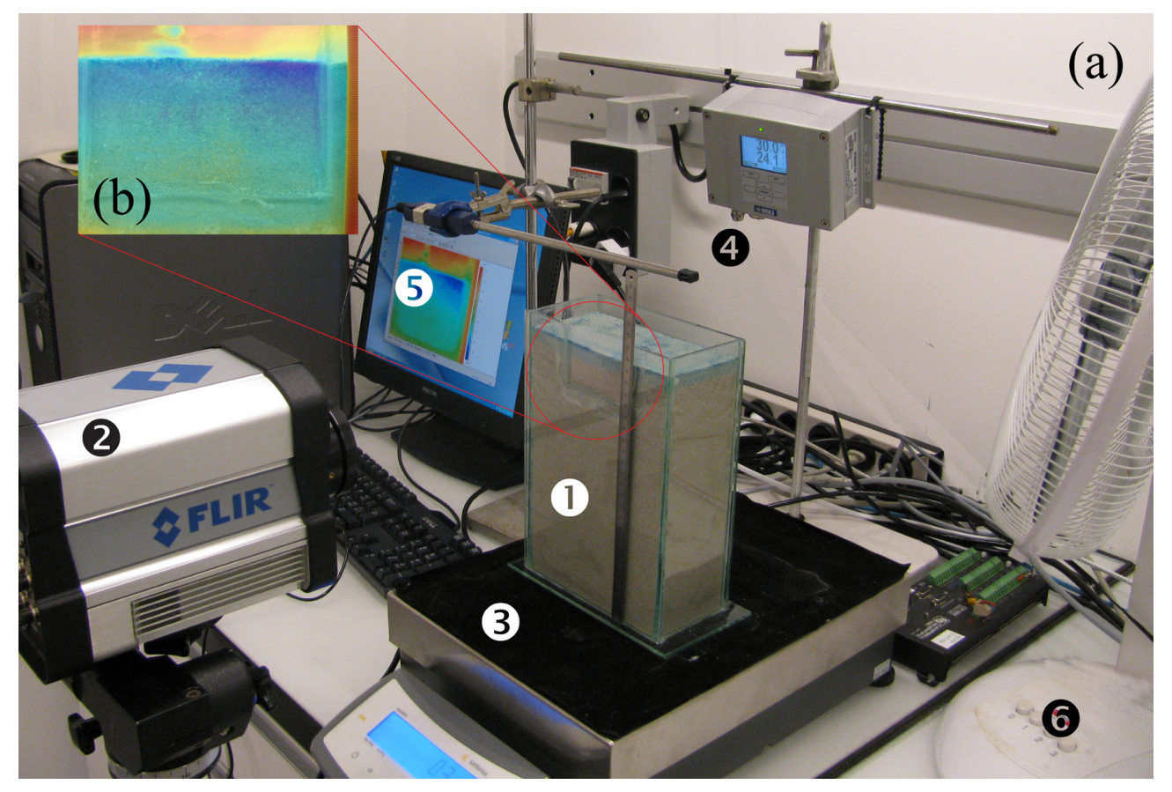

Figure 3: **(a)** Experimental setup for side view IRT imagery beneath an evaporative surface:
(1) Sample with transparent PIR window
(2) IR camera
(3) Balance (32kg±0.1g)
(4) Ambient conditions recorders
(5) PC for data acquisition
(6) fan
(b) IR image of side view temperature distribution

Results and Discussion

- Equation (1) maps spatially and temporally variable surface temperature distribution to a corresponding evaporation rate field (Figure 4a-f)
- Equation (3) yields evaporation curves from different patches of the surface by using only averaged temperature changes (Figure 4h)
- Results shows excellent agreement with balance recorded data (Figure 4h)
- Assuming constant flux $\dot{e}_0$ in equation (2) yields $T(x,z)$ as:

$$T(x,z)=T_\infty-\frac{\rho_wL_w\dot{e}_0b}{B\left(h+4\sigma\varepsilon T_\infty^3\right)}-2\rho_wL_w\dot{e}_0B\sum_{m=1}^{\infty}\frac{\frac{1}{m\pi}\exp\left(-\frac{m\pi z}{B}\right)}{m\pi k_T+B\left(h+4\sigma\varepsilon T_\infty^3\right)}\sin\left(\frac{m\pi b}{B}\right)\cos\left(\frac{m\pi x}{B}\right) \qquad (4)$$

- Knowing (4) and averaging over the whole patch surface, $\dot{e}_0$ can be found to match $T(z)$ with IR data as depicted in Figure 4g

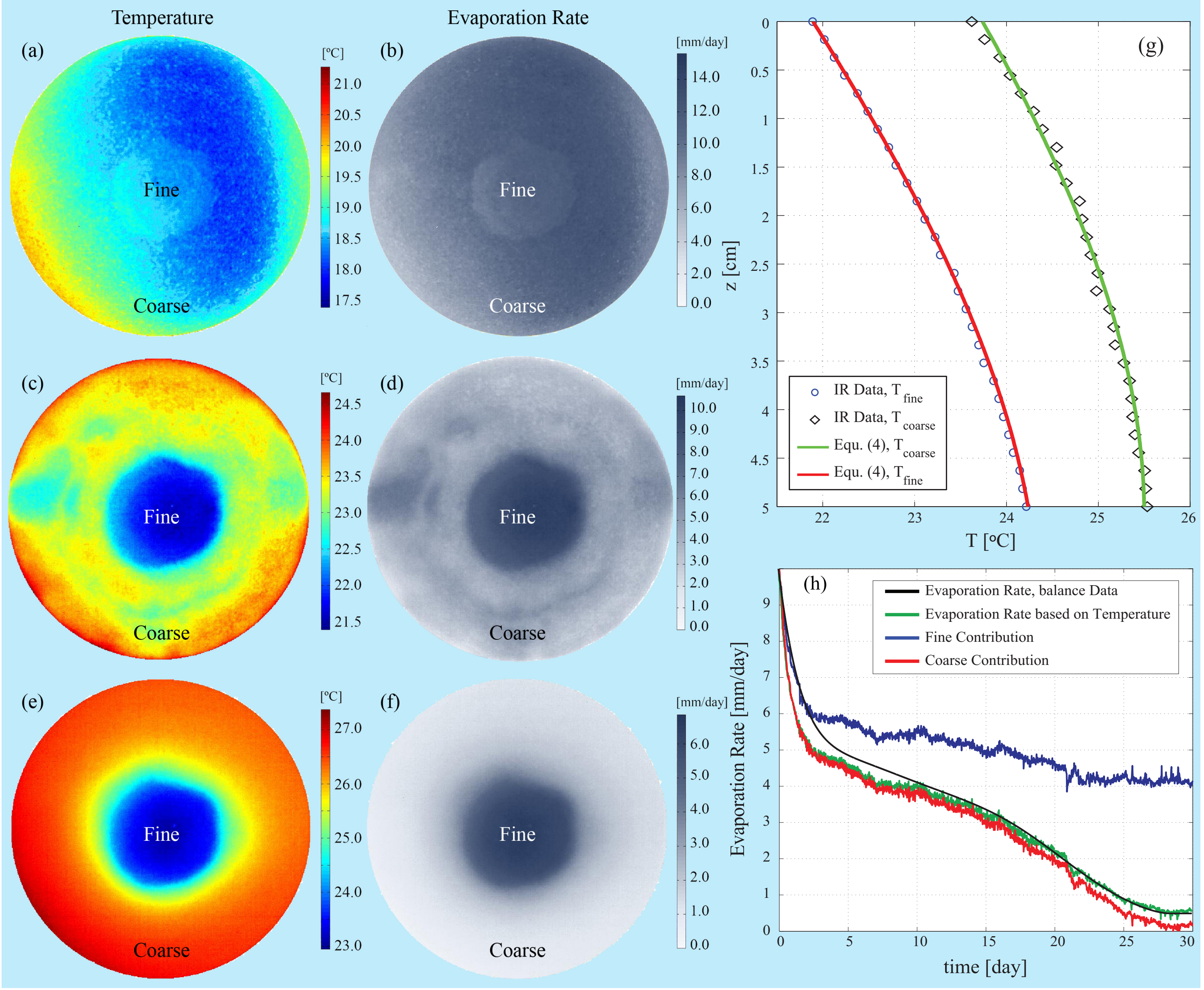

Figure 4: **(a) - (b)** Temperature distribution and evaporation rate resulted from equation (1) at t = 0. **(c) - (d)** Same results at t = 6days. **(e) - (f)** Same results at t = 30days. **(g)** Inversion of averaged form of equation (4) for known $\dot{e}_0$ provides excellent match with side view IR measured subsurface temperature profile **(h)** Comparison of evaporation curves from measured balance data (total for the column) and deduced from surface temperature

Conclusions

- A physically-based model for mass-energy exchanges during evaporation from porous media surfaces was developed
- Use of averaged temperature and dimensionless groups yield a practical method for IR estimation of spatially distributed evaporation
- Prediction of thermal field beneath a surface strengthen evaporation estimation and accounts for inaccessible thermal information
- Side view IR measurements beneath an evaporative surface provides experimental verification for subsurface temperature distribution
- The study provides a sound basis for resolving spatially-variable evaporation fluxes from heterogeneous surfaces at plot and field scales using IR remote sensing

References:

1. Shahraeeni, E. and Or, D., 2010, Temperature Field beneath Evaporating Surfaces Resolved by Infrared Thermography, International J. Heat and Mass Transfer, In Review.
2. Shahraeeni, E. and Or, D., 2010, Thermo-evaporative fluxes from heterogeneous porous surfaces resolved by infrared thermography, Water Resour. Res., In Press, 10.1029/2009WR008455

Acknowledgements:

- This project is funded by the SNF (2000021-113676/1).
- This poster has been prepared for HS6.7: The role of interfaces in flow and transport in porous media session in EGU General Assembly 2010, Vienna, Austria, 2-7 May 2010.
- This poster participates in YSOPP (Young Scientists' Outstanding Poster Paper) Contest.

Schweizerischer Nationalfonds
Fonds national suisse
Swiss National Science Foundation
Fondo nazionale svizzero